ELSEVIER

Biochimica et Biophysica Acta 1329 (1997) 61–73

BIOCHIMICA ET BIOPHYSICA ACTA
BBA

Interlamellar waters in dimyristoylphosphatidylethanolamine–water system as studied by calorimetry and X-ray diffraction

Michiko Kodama [a,*], Hiroyuki Aoki [a], Hiroshi Takahashi [b], Ichiro Hatta [b]

[a] *Department of Biochemistry, Faculty of Science, Okayama University of Science, 1-1 Ridai-cho, Okayama 700, Japan*
[b] *Department of Applied Physics, Nagoya University, Nagoya 464-01, Japan*

Received 13 February 1997; accepted 8 April 1997

Abstract

The number of water molecules incorporated into the interlamellar region in a gel phase of dimyristoylphosphatidylethanolamine (DMPE)–water system containing up to about 40 g% water was estimated by techniques of calorimetry and X-ray diffraction. The calorimetric estimation based upon enthalpy changes of deconvoluted ice-melting peaks revealed that bulk water existing outside lipid bilayers begins to appear although the gel phase is not fully hydrated. The gel phase showed a linear depression of its transition temperature proportional to the amount of freezable waters interposed between bilayers. For a fully hydrated gel phase, the numbers of non-freezable and freezable interlamellar waters estimated by calorimetric analysis were about 2.3 and 3.7 molecules per lipid, respectively. The limiting, total number of interlamellar waters, 6 H_2O/lipid, agreed with that estimated from both the X-ray diffraction data and the absolute specific volume for a DMPE molecule. Furthermore, the analysis for the lamellar intensity data is also consistent with the result of calorimetric analysis. © 1997 Elsevier Science B.V.

Keywords: Dimyristoylphosphatidylethanolamine; Interlamellar water; Differential scanning calorimetry; X-ray diffraction; Electron density profile

1. Introduction

Phosphatidylethanolamine (PE) as well as phosphatidylcholine (PC) constitute the majority of the total phospholipids in biomembranes. However, phase behavior of both lipids in the presence of water fairly differs from each other [1,2]. From this viewpoint, studies of the interaction of lipid and water molecules are the subject of many investigators and the amount of water molecules interposed between lipid bilayers has been estimated by many techniques [3–8]. Of these techniques, the X-ray diffraction method has been the most frequently and widely used, and for many years, a gravimetric method proposed by Luzzati [9] had been used to estimate structural parameters about the bilayers from X-ray repeat distance [10,11]. However, recently, many objections have raised to gravimetrically determining the volume fractions of lipid and water (ϕ_1 and ϕ_w) in the sub cell (a single lipid plus its associated n_w water molecules), on the basis of the assumption that all the water molecules added are preferentially incorporated between the bilayers up to their saturation [5–7,12–15]. Accordingly, applying the Luzzati method depends on whether the assumption is reasonable or

* Corresponding author. Fax: (81) (86) 255-7700.

PII S0005-2736(97)00086-2

not. From the viewpoint of avoiding this uncertainty, Nagle and co-workers have proposed a way of estimating n_w without utilizing the water content of sample [7,16]. Furthermore, in order to promote a more accurate estimation, electron density modeling analysis has been developed and much progress has been made [5,6,14,15].

With a view to evaluating the Luzzati method, the present study investigated how the number of water molecules between the bilayers of DMPE gel phase varies with water content. The number of the interbilayer water molecules was determined from the enthalpy change due to the melting of frozen water obtained by a differential scanning calorimetry (DSC). For the present calorimetric analysis, it is required that the melting enthalpy of frozen bulk water outside the bilayers is estimated as accurately as possible. From this viewpoint, ice-melting DSC curves were analyzed by a deconvolution method according to a computer program. Furthermore, with the purpose of ascertaining calorimetric results, the number of interbilayer water molecules of a fully hydrated DMPE gel phase was estimated from X-ray diffraction data by applying two different methods. One estimation was performed based upon lamellar spacing data and densitometric data [17]. The other estimation was performed from an analysis for the lamellar intensity data according to a strip function model convoluted a Gaussian function, considering that real DMPE bilayers fluctuate due to thermal motion and the interbilayer water molecules penetrate into the head group regions [18–20].

2. Materials and methods

2.1. Materials and sample preparation

1,2-Dimyristoyl-3-*sn*-phosphatidylethanolamine (DMPE) was purchased from Sigma Co. (St. Louis, MO) and used without further purification as thin-layer chromatography of this lipid showed a single spot. The DMPE, which was transferred to the high-pressure crucible cell of a Mettler differential scanning calorimeter (TA-4000, Switzerland), was dehydrated under high vacuum (10^{-4} Pa) at room temperature for at least 3 days until a weight loss was not detected by electroanalysis (Cahn Electrobalance, California). The crucible cell containing the dehydrated DMPE was sealed off in a dry box filled with dry N_2 gas and then weighed by a microbalance (Mettler M3, Switzerland). Samples of the DMPE water mixture ranging, in water content, from 0 to about 40 g% were prepared by successive additions of desired amounts of water to the same dehydrated compound (49.96 mg) by using a microsyringe. Thus, only the weight of water was changed through the preparation of a series of samples of different water contents. The water contents were ascertained by weighing the sample and the cell by microbalance. All the samples were annealed by repeating thermal cycling at temperatures above and below the transition to the liquid crystal phase to ensure homogeneous mixing, until the same transition peak was attained. After that, the samples were cooled to -60°C for the differential scanning calorimetry (DSC). After the DSC, the weight of the sample and the cell was rechecked by microbalance.

For the X-ray diffraction measurement, the sample of 32 g% water was transferred to a capillary noted below.

2.2. Differential scanning calorimetry (DSC)

DSC was carried out with a Mettler TA-4000 apparatus by placing the sample in a high-pressure crucible (pressure resistant to 100 kP/cm^2) and heating it from -60°C to temperatures above transition to the liquid crystal phase at a rate of 1.0°C/min.

2.3. X-ray diffraction

X-ray diffraction measurements were performed with a RU200BEH rotating anode generator (Rigaku, Tokyo, Japan). The optical system has been described elsewhere [21]. The sample was sealed in a fine wall quartz capillary with a 2-mm diameter (Hilgenberg, Malsfeld, Germany). The sample capillary was fixed to a brass hollow holder. Temperature of the sample was controlled within ± 0.1°C by circulating water from a temperature-controlled waterbath (B. Braun, Melsungen, Germany) to the sample mount. X-ray diffraction patterns were recorded on imaging plates with size of 20×25 cm (BAS-III, Fuji Photo Film Co. Ltd., Tokyo, Japan). Digitizing the data on imaging plates was performed on a BAS2000 system (Fuji

Photo Film Co, Ltd., Tokyo, Japan). Diffraction patterns were averaged by azimuthally integrating two-dimensional Debye–Scherrer patterns [22] and were corrected by subtracting the background scattering obtained from the measurements of an empty capillary. The intensities of the lamellar reflections were determined by fitting the observed reflection peaks to Lorentzian line shapes [23]. The diffraction spacings were calibrated by using the lamellar spacings of anhydrous cholesterol (3.39 nm at 20°C) [24,25].

3. Results

3.1. Differential scanning calorimetry

3.1.1. Changes in thermal behavior of lipid and water molecules with an increase in water content

Fig. 1 shows a series of thermal behavior of DMPE for varying water contents at an interval of about 2 g%. The phase transition due to the so-called chain-melting is characterized by either primary or secondary peaks according to water content. The phase transition at water contents lower than 6 g% is characterized by the primary peak (see curves a and b). Above this water content, the primary transition peak is replaced by a newly produced secondary peak, although both peaks are observed at a water content of 8 g% (see curve c). As shown in Fig. 2, the transition temperature of the secondary peak gradually shifts to lower temperatures with increasing water content up to 22 g%, at which it reaches a limiting temperature generally accepted as the transition temperature of the gel-to-liquid crystal phases in excess water. Similar behavior was observed for the width of half-height of the secondary peak, as shown in Fig. 2.

Fig. 3 shows a series of ice-melting peaks at the water contents corresponding to those of Fig. 1. In this figure, the shape of ice-melting peaks changes with increasing water content, although no ice-melting peak is observed at water contents lower than 6 g% (see curves a and b). The absence of ice-melting peak indicates that all the water added exists, most likely, between lipid head groups, which is considered non-freezable interlamellar water [26–28]. Ice-melting peak is first observed when a water content reaches 8 g% (see curve c), at which the secondary

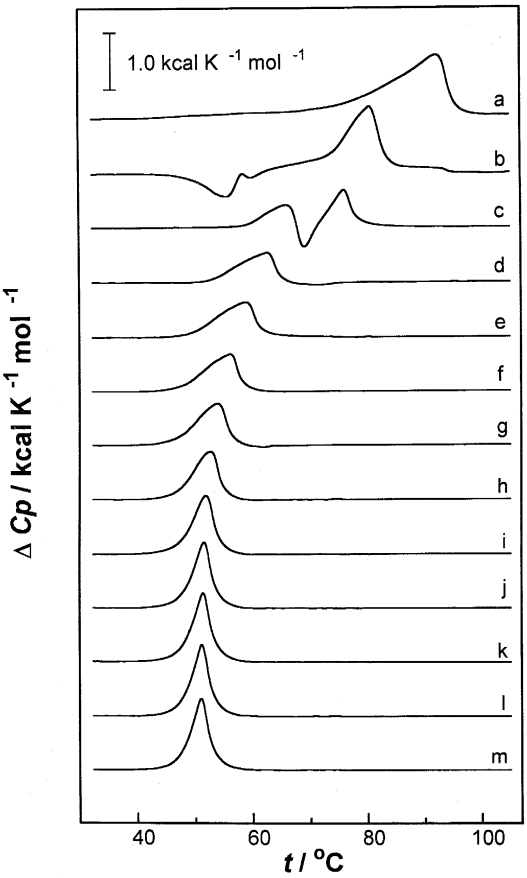

Fig. 1. A series of thermal behaviors of DMPE with increasing water content. Apparent, excess heat capacity (ΔCp) per mol of DMPE is plotted as a function of temperature (t). Water content (g%): (a) 2.25; (b) 6.0; (c) 8.0; (d) 10.2; (e) 12.2; (f) 14.1; (g) 16.1; (h) 18.1; (i) 20.0; (j) 22.0; (k) 25.0; (l) 28.0; (m) 32.0.

transition peak of the lipid first appears. With an increase in water content, the ice-melting peak grows into a broad component extending over a wide temperature range below 0°C (see curves d and e). Based upon our previous papers [26,27], the broad ice-melting peak is suggested to result from freezable water existing between the bilayers, i.e., freezable interlamellar water. Focusing on the simultaneous appearance of both the broad ice-melting peak and the secondary lipid transition peak at the same water content, this fact suggests the key role of the freezable interlamellar water in the appearance of DMPE gel phase. With a further increase in water content (see curves f–m), the broad ice-melting peak is accompanied by a growth of a new sharp peak at around 0°C. The sharp ice-melting peak is considered

to result from bulk water existing outside the bilayers [26,27].

3.1.2. Deconvolution analysis of ice-melting peaks

In order to estimate a melting enthalpy of each of two types of freezable water, i.e., interlamellar water and bulk water, all the ice-melting DSC curves shown in Fig. 3, except that of 8 g% water, were deconvoluted on the basis of a computer program ORIGIN (Microcal Software, Inc.) according to a multiple Gaussian curve analysis. The present deconvolution analysis was performed as follows: (1) minimizing the total number of deconvoluted curves under the condition that the sum of these curves gives a theoretical curve best fitted to the experimental DSC curve; and (2) fixing of both the half-height width and the midpoint temperature of each of the deconvoluted curves throughout all the deconvolutions. Typical results of the deconvolution analysis are shown in Fig. 4A–D. In each panel, resultant deconvoluted curves and a theoretical curve are shown by dotted lines. In Fig. 4A, the ice-melting peak characterized by only the broad component at 10.2 g% water is deconvoluted into three curves I, II and III. Above this water content, as shown in Fig. 4B–D, three deconvoluted curves similar to those of Fig. 4A are followed by a newly deconvoluted curve IV comparable to the sharp component at 0°C. However, the size of the corresponding curves is different and becomes larger with increasing water content. In particular, a significant growth of the deconvoluted curve IV with increasing water content is observed in Fig. 4.

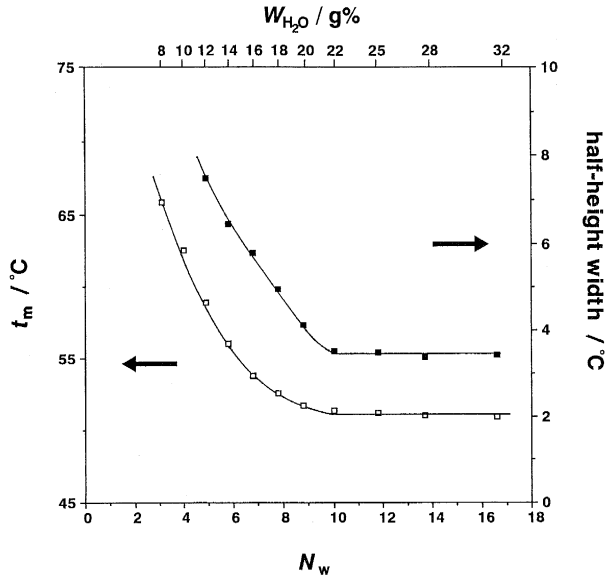

Fig. 2. Variation with increasing water/lipid molar ratio (N_w) of transition temperature (t_m) of gel-to-liquid crystal phases (□) and half-height width of the transition peak (■).

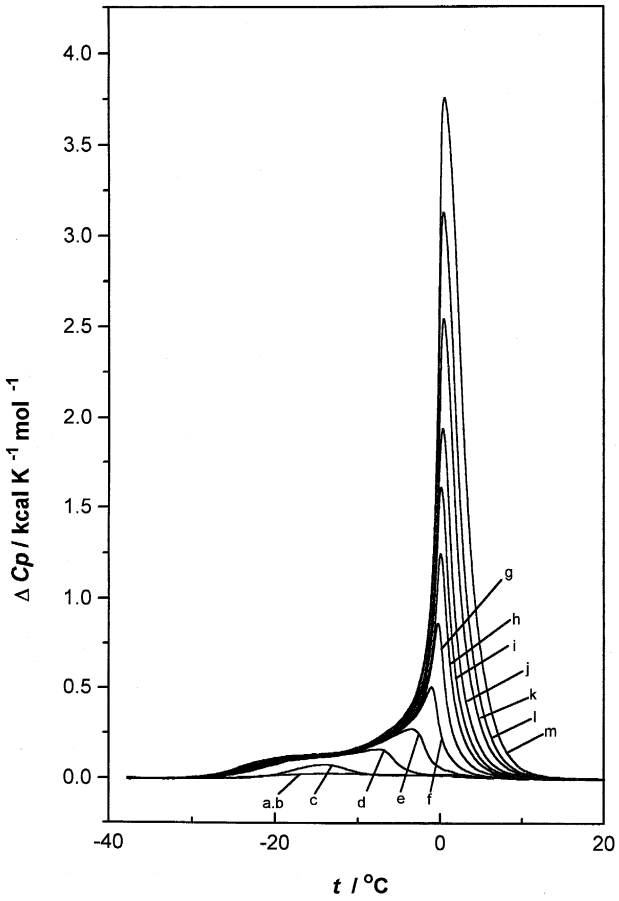

Fig. 3. A series of ice-melting curves for gel phases with increasing water content. Apparent, excess heat capacity (ΔCp) per mol of DMPE is plotted as a function of temperature (t). Water content (g%): (a) 2.25; (b) 6.0; (c) 8.0; (d) 10.2; (e) 12.2; (f) 14.1; (g) 16.1; (h) 18.1; (i) 20.0; (j) 22.0; (k) 25.0; (l) 28.0; (m) 32.0.

Table 1 summarizes enthalpy changes ΔH_1, ΔH_2, ΔH_3 and ΔH_4 of the deconvoluted curves I, II, III and IV per 1 mol of DMPE at different water contents. A water/lipid molar ratio N_w (molar number of waters added to 1 mol of DMPE) corresponding to a water content W_{H_2O} is also given in Table 1. In Fig. 5, the ΔH_1, ΔH_2 and ΔH_3, together with the

sum of these enthalpy changes are plotted against N_w, respectively. The ΔH_1, ΔH_2 and ΔH_3 all increase in proportions of approximately 1:2:1 with increasing N_w. When N_w reaches around 10 (22 g% water), all the enthalpy changes are saturated. Similar behavior is observed for the sum of enthalpy changes, indicating that at around $N_w = 10$, the amount of the freezable interlamellar water reaches a maximum and the gel phase is fully hydrated. The $N_w = 10$ is just the same as the water content, at which both the temperature and the width of half-height for the gel-to-liquid crystal transition peak become independent of water content (see Fig. 2). The sum of enthalpy curve $\Delta H_{(1+2+3)}$ in Fig. 5 increases more and more gently with an increase in N_w over the molar ratio range of 4–10. By extrapolating the sum of enthalpy curve to a lower water content region, N_w at a starting point of this curve is shown to be 2.3 ± 0.2, above which the freezable interlamellar water is furnished. Accordingly, the value of 2.3 water molecules per lipid indicates a limiting number of the non-freezable interlamellar water molecules in the present system. In this contrast, the value of 10 water molecules per lipid at the saturation point of the sum of enthalpy curve is not assigned to a maximum limiting number of the whole (freezable + non-freezable) interlamellar water molecules because the bulk water characterized by the deconvoluted

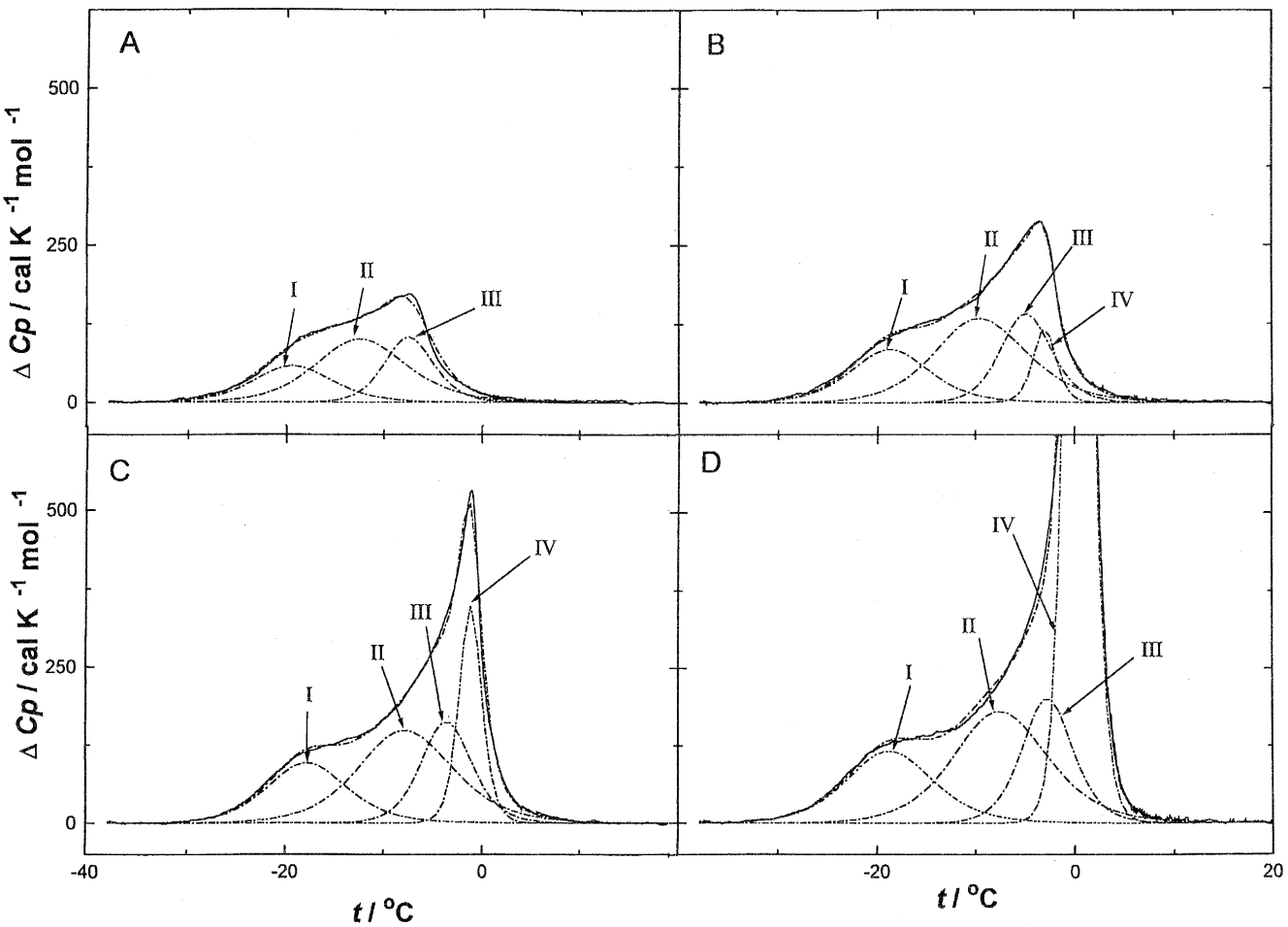

Fig. 4. Deconvolution analysis of ice-melting curves for gel phases at water contents of 10.2 (A), 12.2 (B), 14.1 (C) and 22.0 (D) g%. The deconvolutions were performed on the basis of a computer program attached to a Microcal calorimeter [23]. In each figure, four deconvoluted curves I, II, III and IV as well as a theoretical curve are shown by dotted lines. The apparent, excess heat capacity (ΔCp) per 1 mol of DMPE is plotted as a function of temperature (t).

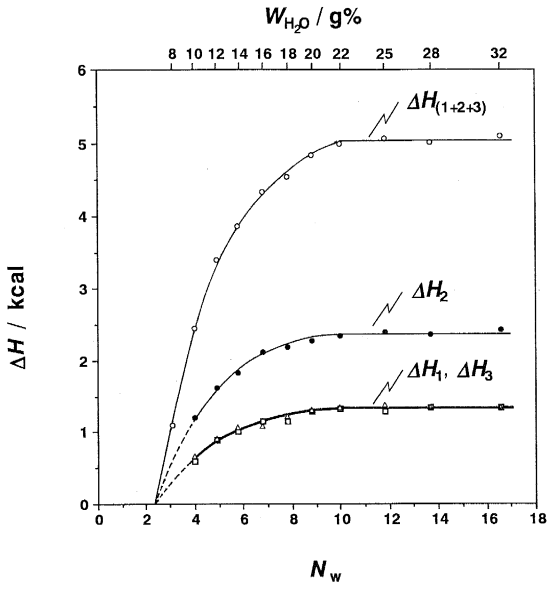

Fig. 5. Variation with increasing water/lipid molar ratio (N_w) of enthalpy changes (ΔH) per 1 mol of DMPE for deconvoluted ice-melting curves I, II and III derived from freezable interlamellar water, together with a sum of these enthalpy changes. ΔH_1, ΔH_2, ΔH_3 and $\Delta H_{(1+2+3)}$ represent enthalpy changes for the deconvoluted curves I, II, III and their sum, respectively. ΔH_1 and ΔH_3 show nearly the same behavior.

curve IV is furnished from the water/lipid molar ratio as low as 4.9, as shown in both Fig. 4B–D and Table 1. Thus, the gel phase, although not fully hydrated, coexists with the bulk water outside the bilayers over the molar ratio range of at least 4–10 at the saturation point.

3.1.3. Estimation of the amount of freezable interlamellar water molecules

Based upon the above-described result, the number of freezable interlamellar water molecules per lipid molecule, $N_{I(f)}$, of the gel phase at different water contents was determined according to the following equation: $N_{I(f)} = N_T - (N_B + N_{I(nf)})$, where N_T is the total number of water molecules added to lipid molecule and equal to N_w; and N_B and $N_{I(nf)}$ are the numbers of bulk and non-freezable interlamellar water molecules per lipid, respectively. At first, another unknown value N_B necessary to determine $N_{I(f)}$ was estimated by assuming that the bulk water exists in the so-called 'free water' characterized by a known value of melting enthalpy, 1.43_6 kcal/mol. In Fig. 6, the enthalpy change ΔH_4 of the deconvoluted curve

Table 1
Enthalpy changes (ΔH_1, ΔH_2, ΔH_3, ΔH_4) of deconvoluted ice-melting curves I, II, III, and IV per 1 mol of lipid, together with the numbers ($N_{I(nf)}$, $N_{I(f)}$, N_B) of non-freezable and freezable interlamellar waters and bulk waters per lipid in gel phases of DMPE–water systems with increasing water contents (W_{H_2O})

	W_{H_2O}/g%	N_w	Enthalpy changes of deconvoluted curves I, II, III and IV per 1 mol of lipid				Numbers of non-freezable, freezable interlamellar waters and bulk waters per lipid		
			ΔH_1/kcal	ΔH_2/kcal	ΔH_3/kcal	ΔH_4/kcal	$N_{I(nf)}$	$N_{I(f)}$	N_B
a	2.3	0.8	0	0	0	0	0.8	0	0
b	6.0	2.2_5	0	0	0	0	2.2_5	0	0
c	8.0	3.1		(1.09) [a]		0	2.3	0.8	0
d	10.2	4.0	0.60	1.19	0.66	0	2.3	1.7	0
e	12.2	4.9	0.88	1.62	0.91	0.25	2.3	2.4	0.2
f	14.1	5.8	1.00	1.84	1.06	1.05	2.3	2.8	0.7
g	16.1	6.8	1.15	2.12	1.07	1.97	2.3	3.1	1.4
h	18.1	7.8	1.15	2.20	1.21	3.04	2.3	3.4	2.1
i	20.0	8.8	1.28	2.27	1.30	4.28	2.3	3.5	3.0
j	22.0	10.0	1.32	2.33	1.33	5.76	2.3	3.7	4.0
k	25.0	11.8	1.29	2.39	1.38	8.21	2.3	3.7	5.8
l	28.0	13.7	1.33	2.36	1.33	11.13	2.3	3.7	7.7
m	32.0	16.6	1.34	2.43	1.34	15.07	2.3	3.7	10.6

N_w represents water/lipid molar ratios corresponding to water content. ΔH_1, ΔH_2, ΔH_3 and ΔH_4 in this table generate a heat capacity function with standard deviations of 0.1–0.3 kcal K^{-1} mol^{-1} for samples at water contents of 10.2–32.0 g%, respectively. Based upon the average standard deviation for heat capacity functions, an average standard deviation for $N_{I(nf)}$, $N_{I(f)}$ and N_B in this table is estimated to be 0.2.

[a] The sum of ΔH_1, ΔH_2 and ΔH_3 is shown because deconvolution is impossible.

IV given in Table 1 is plotted against N_w. To clarify the relationship among N_T, N_B and N_I ($= N_{I(f)} + N_{I(nf)}$) in the present system from the viewpoint of enthalpy, the enthalpy curve given by 1.43_6 N_T is added in Fig. 6. This theoretical curve is based upon the assumption that all the water added is present in the bulk free water. In Fig. 6, the ΔH_4 curve shows a gentle increase over the molar ratio range of 4 (a starting point) to 10, similar to the behavior of $\Delta H_{(1+2+3)}$ curve at the same molar ratio range in Fig. 5. Above $N_w = 10$, the ΔH_4 curve increases linearly and parallel to the theoretical curve, indicating that the enthalpy difference between both curves given by 1.43_6 ($N_T - N_B$) equal to 1.43_6 N_I is the same at molar ratios higher than 10. Thus, the number of the whole interlamellar water molecules is revealed to be the same above $N_w = 10$, which is consistent with the result obtained from the $\Delta H_{(1+2+3)}$ curve in Fig. 5. The maximum limiting number of the whole interlamellar water molecules was determined by extrapolating the straight ΔH_4 curve above $N_w =$ 10 to lower molar ratios. As shown in Fig. 6, the extrapolated line intersects with the abscissa at $N_w =$ 6.0 ± 0.2, indicating that the limiting number of the whole interlamellar water molecules is approximately 6 molecules per lipid. Accordingly, the limiting number of freezable interlamellar water molecules is estimated to be approximately $3.7(= 6.0 - 2.3)$ molecules per lipid. On the other hand, the number of the whole interlamellar water molecules at molar ratios ranging from 4 to 10 was determined by dividing the enthalpy difference between the theoretical and ΔH_4 curves by 1.43_6. As to molar ratios lower than 4 in the absence of the bulk water, the whole number was calculated by dividing the theoretical enthalpy value by 1.43_6. The resultant values of $N_{I(nf)}$, $N_{I(f)}$ and N_B are given for varying water contents in Table 1.

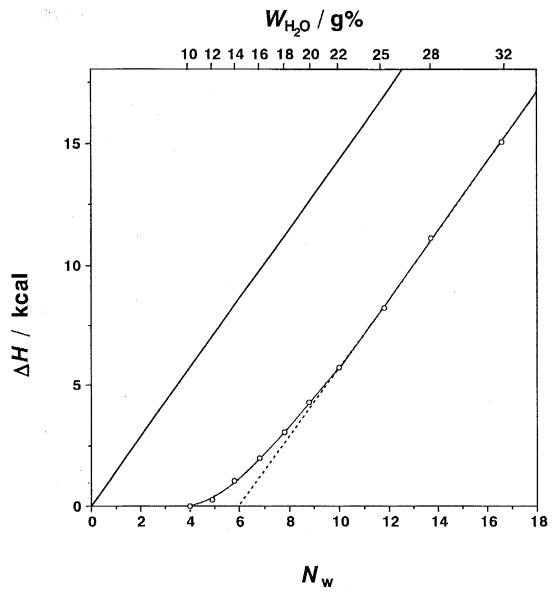

Fig. 6. Variation with increasing water/lipid molar ratio (N_w) of enthalpy changes (ΔH) per 1 mol of DMPE for deconvoluted ice-melting curve IV derived from bulk water. The bold line shows a theoretical curve obtained from the melting enthalpy of hexagonal ice.

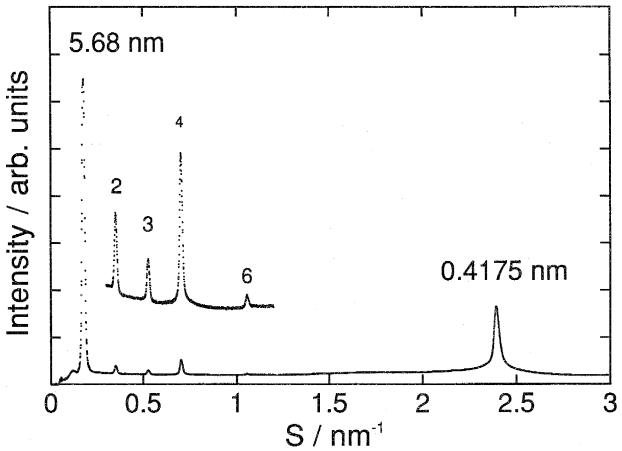

Fig. 7. X-ray diffraction patterns for a fully hydrated DMPE in gel phase (20°C). S is defined by $2\sin\theta/\lambda$, where 2θ is the scattering angle and λ is the wavelength of X-ray. The exposure time was 6 h. For $0.3 < S < 1.2$, the plot with a 10-fold expanded scale is also shown.

3.2. X-ray diffraction

3.2.1. X-ray diffraction pattern

Fig. 7 shows the diffraction pattern for a fully hydrated DMPE in the gel phase (20°C). The lamellar and the wide-angle spacings are 5.68 (± 0.01) nm and 0.4175 (± 0.0005) nm, respectively. The spacings are similar to those previously reported by Seddon et al. [10]. The lamellar reflections were observed up to the sixth order. For the lamellar reflections of the first to sixth orders, the normalized amplitudes of the structure factors were determined to be 100.0, 9.01, 11.27, 72.90, 0.00, and 13.67,

respectively, where these magnitudes were normalized by that of the first-order reflection. A single sharp reflection in the wide-angle region indicates that the hydrocarbon chains in the gel phase are packed in a hexagonal lattice and oriented parallel to the normal of the bilayer [29].

3.2.2. Estimation of the amount of interlamellar water based upon the observed spacings and the reported density

From the wide-angle spacing (d), the area occupied by a DMPE molecule at the surface of the bilayer was calculated to be 0.4025 nm^2 ($=4d^2/\sqrt{3}$). Then, from this value and the lamellar spacing, the volume occupied by a fully hydrated DMPE molecule and its associated water molecules in interlamellar was calculated to be 1.143 nm^3 [$=(0.4025\ \text{nm}^2)\times\{(5.68\ \text{nm})/2\}$]. On the other hand, the volume of the fully hydrated DMPE molecule has been reported to be 0.964 nm^3 (0.893 ($\pm$0.005) ml/g) in a recent densitometric study [17]. Therefore, the total volume of water associated with a DMPE molecule in the gel phase was estimated to be 0.179 nm^3 [$=(1.143\ \text{nm}^3)-(0.964\ \text{nm}^3)$]. On the assumption that the volume of a water molecule associated with the gel-state DMPE is equal to that in bulk free water, i.e., 0.030 nm^3, the number of water molecules associated with a DMPE molecule in the gel phase was estimated to be 5.97 ($\pm$0.04).

3.2.3. Estimation of the amount of interlamellar water based upon the observed lamellar intensities

In this analysis, the number of water molecules between bilayers was directly estimated from only X-ray diffraction data, using a model for the electron density profiles of the DMPE–water system. Simple strip models have been used to analyze the structure of lipid bilayers [14,22,30]. In the simple strip models, the electron density of a bilayer structure is represented by a sequence of constant electron densities. We considered a three-strip model for the electron density of the DMPE bilayers in the unit cell. The bilayer was divided into the three parts with constant electron density, namely, terminal methyl, methylene, and headgroup. X-ray [31] and neutron [32] diffraction studies have revealed that the molecular conformation of DMPE or DPPE in the gel phase is well-expressed by that of the DLPE/acetic acid

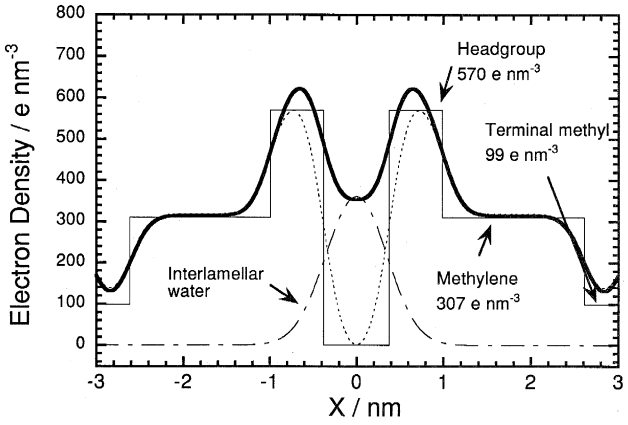

Fig. 8. Thick solid line curve shows the model for the electron density model of the DMPE–water system in the gel phase with the best-fit parameters. This model consists of a Gaussian function representing the interlamellar water (dot–dash line) and a smeared strip model for the DMPE bilayers (dotted line). The strip model (thin solid line) consists of three parts: terminal methyl, methylene, and headgroup. Smearing was performed with the convolution of a Gaussian function and the simple strip model.

crystal [33,34]. From the crystallographic data, we estimated the lengths as 0.225, 1.625, and 0.61 nm for terminal methyl, methylene, and headgroup regions, respectively (see Fig. 8). The electron density for each region was calculated from the number of electrons and the volume occupied by the above regions. The area occupied by a lipid calculated from the wide-angle data as described above was used to calculate the volume. The levels of the electron density for each region are presented in Fig. 8 (see a three-strip model shown by thin solid line). In a real electron density profile of phospholipid bilayer, there is no clear jump among the each part as shown by a thin solid line in Fig. 8. In addition, a real bilayer fluctuates due to thermal motion. In order to reflect these matters in the present model, the jumps in the electron density of the strip model were smeared in terms of the convolution of a Gaussian function. This corresponds to the treatment that atomic form or structure factors are multiplied by the Debay–Waller temperature factor [18,20,35]. The electron density of the interlamellar water was also expressed by a Gaussian function (see a dot–dash line in Fig. 8). Thereby, the penetration of water into the DMPE bilayer region was taken into account in the consideration. The center of the Gaussian function for water

was taken at the zero position (see Fig. 8). The width and height of the Gaussian function for the interlamellar water, and the width of the Gaussian function convoluted to the strip model of the bilayer were taken as parameters. The optimal values of these three parameters were determined by searching the minimum of a crystallographic R factor defined by

$$R = \frac{\sum \| F_c(h) | - K | F_o(h) \|}{\sum K | F_o(h) |}, \quad (1)$$

where K is a scaling factor given by

$$K = \frac{\sum | F_c(h) |}{\sum | F_o(h) |}, \quad (2)$$

where $F_c(h)$ is the structure factor calculated from the model and $|F_o(h)|$ is the absolute value of the observed normalized structure factor. The smaller value of the R factor implies that the model is more reasonable for explaining the observed lamellar intensities. We used the minimization program developed by Okumura [36]. The program is constructed based upon a simplex algorithm [37]. As a result, the value of the R factor became minimum ($R = 0.18$), when the height of the Gaussian function of the water was 360 e nm^{-3} and the widths of the Gaussian function convolved to the strip model of the bilayer and the Gaussian function representing the interlamellar water were 0.26 and 0.49 nm, respectively. The number of water per lipid can be estimated to be ~ 6.4 from the integration of the Gaussian function of the interlamellar water in the model with the best-fit parameters. This analysis for the lamellar intensities also supports the result of 5.97 in the previous section. In the model with the best-fit parameters, the interlamellar water penetrates near the glycerol part of the DMPE bilayer (Fig. 8). This is in good agreement with the results of neutron diffraction studies [35,38,39] and a combined study of X-ray and neutron diffraction data [19].

However, it should be pointed out that an equally small value for the R was obtained with a few waters with a narrow distribution. In such a case, an extremely low level in the electron density appeared at the boundary part between the headgroup and the interlamellar water. Hence, this case should be discarded because of the unrealistic distribution of water. By using a preliminary simple strip model (the detailed procedure was described elsewhere [15]), the number of water per lipid was also estimated to be about 6 in the interlamellar region for the fully hydrated gel phase. In the simple model, the electron density of interlamellar water region was also expressed by a flat distribution and the penetration of water into the bilayers was not considered. In the analysis, we took the number of water molecule as a parameter. Recently, Katsaras et al. [40] have reported that in their analysis to determine the water distribution in lipid–water systems based upon only X-ray diffraction data, equally good fits were also obtained for unrealistic water distributions. Then, as Katsaras et al. [40] described, one of the best methods to determine the water distribution in lipid bilayer systems would be neutron diffraction measurements or it would be very useful to combine X-ray and neutron diffraction data.

4. Discussion

Compared with our previous study [8], the present study makes certain improvement in the water content of samples. In our previous study, a dehydrated DMPE as a starting material was prepared by dehydration at room temperature under high vacuum (10^{-4} Pa) for 1 day. Before starting the present study, the dehydration period was checked by electrobalance. Based upon a result of the electrobalance, dehydration in the present study was performed for 3 days until a weight loss was not detected. Another improvement was made in the deconvolution analysis of ice-melting peak. Thus, in the present study, the deconvoluted curves III and IV have been separated from each other by an independent Gaussian curve, as shown in Fig. 4, although in our previous paper, two of these curves were combined with a single Gaussian curve [8]. This is because a conversion of DMPE gel phase into a semi-crystalline structure by a special annealing treatment over the period of 7 days involves a growth of the ice-melting peak just comparable to the deconvoluted curve III of Fig. 4. Therefore, it became impossible to ignore the existence of this deconvoluted curve.

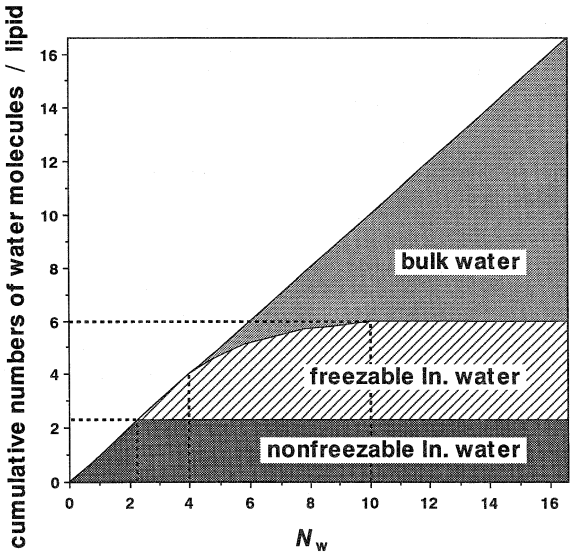

Fig. 9. Variation with increasing water/lipid molar ratio (N_w) of cumulative numbers of non-freezable, freezable interlamellar waters and bulk waters per lipid shown in Table 1.

Based upon the results obtained in the present study, we will discuss the following main points.

4.1. Calorimetric analysis of water molecules in different bonding modes

Fig. 9 schematically shows the result of calorimetric analysis of water molecules in different bonding modes in the present gel system. In Fig. 9, the cumulative numbers ($N_{I(nf)} + N_{I(f)} + N_B$) of non-freezable and freezable interlamellar water molecules and bulk water molecules per lipid given in Table 1 are plotted against N_w. The result is summarized as follows: (1) below 2.3 molar ratios, there is only the non-freezable interlamellar water tightly bound to lipid head groups in a bilayer and this non-freezable water induces the primary transition peak of the lipid; (2) at the molar ratio range of 2.3–4.0, all the water added beyond 2.3 molar ratios exists in the freezable interlamellar water loosely bound to the head groups between the bilayers, and this freezable water induces the secondary transition peak of the lipid, the temperature of which is lowered with increasing water content, finally to the limiting transition temperature of DMPE gel phase [1,2]; (3) above 4.0 up to 10 molar ratios, some of the water added beyond 4.0 molar ratios exists in the freezable interlamellar water and the remainder exists in the bulk water, indicating that the gel phase, not being fully hydrated, coexists with the bulk water; and (4) above 10 molar ratios, at which the maximum uptake of the freezable interlamellar water is achieved, all the water added beyond $N_w = 10$ exists in the bulk water, indicating that the fully hydrated gel phase and bulk water coexist.

The most noticeable result on Fig. 9 is a discrepancy between values of the maximum cumulative number of interlamellar water molecules ($N_{I(nf)} + N_{I(f)} = 6$) and the water/lipid molar ratio ($N_w = 10$) at the saturation point. Based upon the above-discussed result, it becomes apparent that this discrepancy is caused by the bulk water which begins to appear from a molar ratio as low as around 4, although the maximum uptake of interlamellar water is not achieved. Accordingly, the relationship of $N_{I(nf)} + N_{I(f)} = N_w$ attained at molar ratios below 4 fails over the molar ratio range of 4–10 of the saturation point. A similar distribution curve of the water molecules was observed for PC and PG systems of different head groups (data not shown). Furthermore, by Klose et al. [12], the distribution of water molecules comparable to the result of Fig. 9 has been reported for the liquid crystal phase on the basis of X-ray diffraction data. In regard to this phenomenon, many comments of other workers [5–7,12–15] have been offered to the Luzzati method [9] so far accepted as the most representative one to estimate structural parameters of the bilayer systems from X-ray diffraction data [10,11]. Thus, by these workers, it has been pointed out that the problem of the Luzzati method is to estimate the volume fractions of lipid and water in a sub-cell from the water content of sample, on the basis of the assumption that all the water added below the saturation point exists between the bilayers. From this viewpoint and as a method without utilizing the water content, electron density modeling analysis has made rapid progress [5,6,14,15,22,30]. Again, focusing on the Luzzati method in connection with Fig. 9, our present result apparently indicates that the assumption adopted in the Luzzati method is not varied over the water/lipid molar ratio range of 4–10 comparable to $N_{I(nf)} + N_{I(f)} \neq N_w$ and therefore, the application of the Luzzati method is limited to the molar ratios below $N_w = 4$.

Again, focusing on the characteristic water distribution in water/lipid molar ratio range of $20 \sim 40$

for the liquid crystal phase of egg lecithin–water system reported by Klose et al. [12], we should refer to a location of the present bulk water coexisting with a partially hydrated gel phase over the molar ratio range of 4–10 shown in Fig. 9 (the corresponding molar ratio range is 8 ~ 17 for DMPC–water system). On the basis of a structural change of stacked bilayer planars into liposome-like structure which proceeds gradually over the molar ratio range of 20–40, Klose et al. have suggested the existence of water locating in regions between adjacent liposomes or in their internal cores, but not intercalated between bilayers. The same idea has been proposed by other workers [13,15]. Under such situations, the water could be expected to behave as bulk water. Accordingly, it seems likely that the appearance of the bulk water in the molar ratio range of 4 ~ 10 for the present system, although not for the liquid crystal phase, is related to a certain conversion of DMPE planar structure, which is characterized by a gently decreasing transition temperature (t_m) shown in Fig. 2. Our important conclusion is that before the achievement of fully hydrated gel and/or liquid crystal phases, there is a specific water concentration range where only a part of water added is incorporated between the bilayers and the other is present in bulk-like water, most likely, intercalated between liposomes.

Another point of attention which should be paid by us is the equilibrium problem closely related to both sample preparation and annealing procedure. In this connection, Klose et al. [12] and Gawrisch et al. [13] have reported that the water in samples under consideration is not homogeneously distributed, indicating that the samples are not in the thermodynamic equilibrium state. However, it has also been reported [12] that a prolonged storage of the samples causes no change in the water distribution of the liquid crystal phase. In sample preparation of the present study, the repeat thermal cycling was adopted up to at least 5 times until the same peaks for both the lipid transition and ice-melting are observed. Furthermore, in the present study, with a view to preparing a series of samples of different water contents, a minute amount of water was successively added to the same dehydrated lipid of a starting material. If a sample at a desired water content is prepared by adding a desired amount of water, all at once to the dehydrated lipid, the thermal cycling up to 30 times is necessary to get

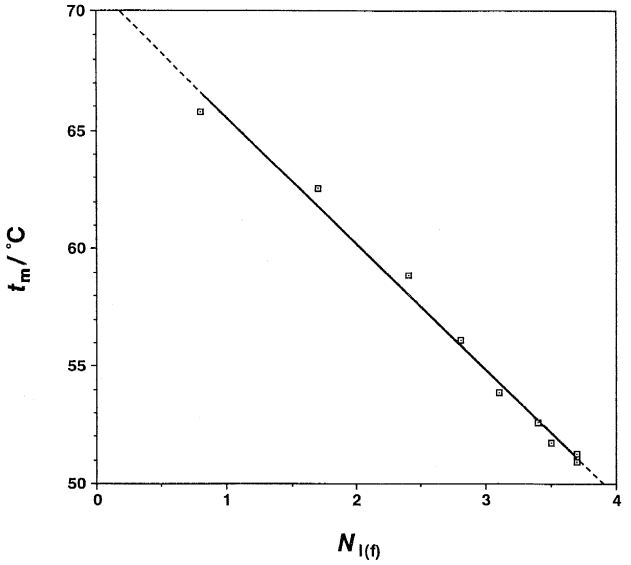

Fig. 10. Variation with increasing number ($N_{I(f)}$) of freezable interlamellar waters per lipid of gel-to-liquid crystal transition temperature (t_m).

an unchanged transition peak. As discussed above, however, by annealing over periods of 7 days, all the gel phases gradually converted into more stable crystalline states (discussed in the next paper), which is different from the case of the liquid crystal phase. Based upon this fact, the present gel system is revealed to stay in the meta- or non-equilibrium state for a considerable period of time.

4.2. Role of the freezable interlamellar water

We discussed above that the present gel phase is induced by the freezable interlamellar water. In this connection, Fig. 2 reveals that the transition temperature of the gel phase (t_m) goes down more gently with increasing molar ratio ranging from 4 to 10, noted in Fig. 9. To clarify the correlation between the freezable interlamellar water and the gel phase, the t_m in Fig. 2 was plotted against $N_{I(f)}$ given in Table 1. In Fig. 10, the result shows a linear relationship between the t_m and $N_{I(f)}$ given by $t_m = -5.3\ N_{I(f)} + 70.8$, indicating that an increment of one molecule of the freezable interlamellar water per lipid depresses the transition temperature by 5.3°C. This suggests that the freezable interlamellar water is a predominant determinant in the lipid lateral packings and interactions of the gel phase. So, the gel phase and the

freezable interlamellar water simultaneously appear at around $N_w = 3$ and in addition, the limiting uptake of this water and the limiting transition temperature for the gel phase are achieved at the same water content around $N_w = 10$.

4.3. Comparison of the present result with that of PE–water systems

In the present calorimetric analysis, six molecules of interlamellar waters per lipid were estimated for the fully hydrated gel phase. The limiting number agrees with the results estimated from the two different analyses for X-ray diffraction data.

Let us compare the present results for the fully hydrated DMPE in the gel phase with that for the other fully hydrated diacyl-PEs with different chain length [7,16] or dialkyl-PE [10,41]. For many PEs in the gel phase, the number of water molecules has been reported to be about 6 which is in good agreement with the present value, except for the estimation in diarachinoyl-PE (DAPE) [10]. As Seddon et al. [10] have discussed, the greater hydration of DAPE in comparison with the other PEs is due to the fact that the water-interface area per molecule for DAPE is larger than that of the other PEs, owing to the tilt of a hydrocarbon chain. Then, the arrangement or the orientation of the headgroup of DAPE differs from that of the other PEs. The fact that the hydration in the gel phase is almost the same for various PEs in which their hydrocarbon chains are normal to the bilayer surface, leads to the conclusion that the hydration for PEs in the gel phase depends on the structure of the headgroup. Namely, both the chain length and the difference of linking the chain to a glycerol backbone does not affect the hydration of PEs in the gel phase.

Acknowledgements

We gratefully acknowledge the High Intensity X-ray Diffraction Laboratory of Nagoya University for the use of the BAS2000 system and also Mr. T. Hikage for his technical assistance with this system. This work is supported in part by Grants-in-Aid for General Scientific Research (07408018 and 07640781) from Ministry of Education, Science and Culture, Japan (1995).

References

[1] D.A. Wilkinson, J.F. Nagle, Biochemistry 20 (1981) 187–192.
[2] J.M. Boggs, Biochim. Biophys. Acta 906 (1987) 353–404.
[3] M.J. Ruocco, G. Shipley, Biochim. Biophys. Acta 691 (1982) 309–320.
[4] G. Cevc, D. Marsh, Biophys. J. 47 (1985) 21–31.
[5] T.J. Mclntosh, S.A. Simon, Biochemistry 25 (1986) 4058–4066.
[6] T.J. Mclntosh, S.A. Simon, Biochemistry 25 (1986) 4948–4952.
[7] J.F. Nagle, M.C. Wiener, Biochim. Biophys. Acta 942 (1988) 1–10.
[8] M. Kodama, H. Inoue, Y. Tsuchida, Thermochim. Acta 266 (1995) 373–384.
[9] V. Luzzati, in: Chapman (Ed.), Biological Membranes, Vol. 1, Academic Press, London, 1968, pp. 71–124
[10] J.M. Seddon, G. Cevc, R.D. Kayer, D. Marsh, Biochemistry 23 (1984) 2634–2644.
[11] R.P. Rand, V.A. Parsegian, Biochim. Biophys. Acta 988 (1989) 351–376.
[12] G. Klose, B. König, H.W. Meyer, G. Schulze, G. Degovics, Chem. Phys. Lipids 47 (1988) 225–234.
[13] K. Gawrisch, W. Richter, A. Möps, P. Balgavy, K. Arnold, G. Klose, StudiaBiophys. 108 (1985) 5–16.
[14] M.C. Wiener, R.M. Suter, J.F. Nagle, Biophys. J. 55 (1989) 315–325.
[15] J.F. Nagle, R. Zhang, T. Stephanie-Nagle, W. Sun, H.I. Petrache, R.M. Suter, Biophys. J. 70 (1996) 1419–1431.
[16] M.C. Wiener, S. Tristram-Nagle, D.A. Wilkinson, L.E. Campbell, J.F. Nagle, Biochim. Biophys. Acta 938 (1988) 135–142.
[17] R. Koynova, H.-J. Hinz, Chem. Phys. Lipids 54 (1990) 67–72.
[18] G. Zaccai, G. Buldt, A. Seelig, J. Seelig, Proc. Natl. Acad. Sci. USA 72 (1975) 376–380.
[19] M.C. Wiener, S.H. White, Biophys. J. 61 (1992) 434–447.
[20] H. Takahashi, T. Yasue, K. Ohki, I. Hatta, Biophys. J. 69 (1995) 1464–1472.
[21] H. Takahashi, I. Hatta, P.J. Quinn, Biophys. J. 70 (1996) 1407–1411.
[22] P.J. Quinn, H. Takahashi, I. Hatta, Biophys. J. 68 (1995) 1374–1382.
[23] H. Takahashi, S. Matuoka, S. Kato, K. Ohki, I. Hatta, Biochim. Biophys. Acta 1069 (1991) 229–234.
[24] H.G. Shieh, L.G. Hoard, C.E. Nordman, Nature 267 (1977) 287–289.
[25] C.R. Loomis, G.G. Shipley, D.M. Small, J. Lipid Res. 20 (1979) 525–535.
[26] M. Kodama, Thermochim. Acta 109 (1986) 81–89.
[27] M. Kodama, H. Hashigami, S. Seki, J. Colloid Interface Sci. 117 (1987) 497–504.
[28] M. Kodama, S. Seki, Adv. Colloid Interface Sci. 35 (1991) 1–30.
[29] A. Tardieu, V. Luzzati, F.C. Reman, J. Mol. Biol. 75 (1973) 711–733.

[30] C.R. Worthington, Biophys. J. 9 (1969) 222–234.
[31] P.B. Hitchcock, R. Mason, G.G. Shipley, J. Mol. Biol. 904 (1975) 297–299.
[32] G. Büldt, J. Seelig, Biochemistry 19 (1980) 6170–6175.
[33] P.B. Hitchcock, R. Mason, K.M. Thomas, G.G. Shipley, Proc. Natl. Acad. Sci. USA 71 (1974) 3036–3040.
[34] M. Elder, P.B. Hitchcock, R. Mason, G.G. Shipley, Proc. Roy. Soc. London, Ser. A 354 (1977) 157–170.
[35] N.P. Franks, W.R. Lieb, J. Mol. Biol. 133 (1979) 469–500.
[36] H. Okumura, Introduction to Data Analysis by Personal Computer, Gijitsu Hyoron sha, Tokyo, 1986, (in Japanese)
[37] J.A. Nelder, R. Meade, Computer J. 7 (1965) 308–313.
[38] D.L. Worcester, N.P. Franks, J. Mol. Biol. 100 (1976) 359–378.
[39] S.A. Simon, T.J. McIntosh, R. Latorre, Science 216 (1982) 65–67.
[40] J. Katsaras, K.R. Jeffrey, D.S.-C. Yang, R.M. Epand, Biochemistry 32 (1993) 10700–10707.
[41] J.M. Seddon, J.M. Hogan, N.A. Warrender, E. Pebay-Peyroula, Progr. Colloid Polym. Sci. 81 (1990) 189–197.